

Zeitschrift: IABSE congress report = Rapport du congrès AIPC = IVBH
Kongressbericht

Band: 10 (1976)

Artikel: Fatigue design of welded joints in trussed legs of offshore jack-up
platform

Autor: Kurobane, Y. / Mitsui, Y. / Atsuta, T.

DOI: <https://doi.org/10.5169/seals-10444>

Nutzungsbedingungen

Die ETH-Bibliothek ist die Anbieterin der digitalisierten Zeitschriften auf E-Periodica. Sie besitzt keine Urheberrechte an den Zeitschriften und ist nicht verantwortlich für deren Inhalte. Die Rechte liegen in der Regel bei den Herausgebern beziehungsweise den externen Rechteinhabern. Das Veröffentlichen von Bildern in Print- und Online-Publikationen sowie auf Social Media-Kanälen oder Webseiten ist nur mit vorheriger Genehmigung der Rechteinhaber erlaubt. [Mehr erfahren](#)

Conditions d'utilisation

L'ETH Library est le fournisseur des revues numérisées. Elle ne détient aucun droit d'auteur sur les revues et n'est pas responsable de leur contenu. En règle générale, les droits sont détenus par les éditeurs ou les détenteurs de droits externes. La reproduction d'images dans des publications imprimées ou en ligne ainsi que sur des canaux de médias sociaux ou des sites web n'est autorisée qu'avec l'accord préalable des détenteurs des droits. [En savoir plus](#)

Terms of use

The ETH Library is the provider of the digitised journals. It does not own any copyrights to the journals and is not responsible for their content. The rights usually lie with the publishers or the external rights holders. Publishing images in print and online publications, as well as on social media channels or websites, is only permitted with the prior consent of the rights holders. [Find out more](#)

Download PDF: 23.02.2026

ETH-Bibliothek Zürich, E-Periodica, <https://www.e-periodica.ch>

Fatigue Design of Welded Joints in Trussed Legs of Offshore Jack-Up Platform

Calcul à la fatigue des joints soudés de colonnes dans les plates-formes auto-élévatrices

Bemessung gegen Ermüdung von geschweißten Stößen in Stützen von selbsthebenden Bohr-Plattformen

Y. KUROBANE

Professor

Kumamoto University
Kumamoto, Japan

Y. MITSUI

Associate Professor

T. ATSUTA

Kawasaki Heavy Industries Ltd.
Kobe, Japan

S. TOMA

1. Description of Structure

The structure under study is a jack-up drilling platform with 3 legs. The legs support a hull measuring 60 x 48 x 7.2 m and of about 6800 tons in weight at intervals of 38.5 m in center to center dimensions (See Fig. 1). The maximum operating sea depth is 90 m. Each leg consists of 4 chords, tubular braces and ties, which constitute a space truss of 119 m in height with a cross section of 7 x 7 m.

Four tubular braces and one tubular tie are framed into each of the corner joints in the chords, which gives a three dimensional complex joint configuration (See Fig. 2). The materials for the chords and tubular members have the tensile strengths of 80 kg/mm² and 60 kg/mm², respectively.

2. Estimation of Stress Concentration Factors in Joints

The ASKA program was used for the elastic stress analysis on the corner joint of the 3 dimensional trussed leg. The model joint for the analysis has only four braces (namely, the tie is omitted) attached at extended positions on the chord surfaces. Fig. 3 shows the finite element mesh and the principal stresses obtained as a result of calculations.

Calculations were carried out for the two most severe load cases, the one is that shown in Fig. 3 and the other has concentrated horizontal forces of 1,885 ton in total acting on the two outstanding teeth of the rack in addition to the member forces in the first case. The stress concentrations occurred at the points along the junctions of the braces and the chord, which are indicated by a mark o in Fig. 3. The peak stresses and the stress concentration factors are shown in Table 1.

According to the response analysis of the structure the severest stresses are generated at the ends of the braces. The stress distribution at these hot spot areas is depicted in Fig. 4, which is a best-fit curve of the stresses obtained by the analyses and is shown in terms of the "local stress / average member stress".

A series of fatigue tests on model joints were also performed. The models, made of low carbon structural steel, have two planar braces and a scale of about 1/4 of the actual joints. The three different types of joints were tested (See Fig. 5 and Table 2). The hot spots in these joints are the points at the weld toes in the brace walls as indicated by a mark • in Fig. 5. The fatigue cracks

were invariably initiated at these points.

Prior to fatigue testing the strains at the hot spot areas were measured by 5 strain gages with the gage length of 2 mm. The hot spot strains were estimated by an extrapolation procedure as illustrated in Fig. 4. Because the estimated hot spot strains were in the inelastic range, the elastic stress concentration factors K_t 's were deduced from them by making use of the

Neuber's formula[1],

$$K_t = \sqrt{K_\sigma K_\epsilon} \quad (1)$$

where K_σ and K_ϵ are the stress and strain concentration factors in the inelastic range. Because K_ϵ is the hot spot strain divided by the nominal strain and can be written as

$$K_\epsilon = \Delta\epsilon / \Delta\epsilon_n = \Delta\epsilon / (\Delta\epsilon_{na} + \Delta\epsilon_{nb}) \quad (2)$$

Eq. (1) can be rewritten as

$$K_t = \sqrt{\Delta\sigma \Delta\epsilon / E \Delta\epsilon_n^2} \quad (3)$$

where $\Delta\sigma$ and $\Delta\epsilon$ are the hot spot stress and strain ranges, $\Delta\epsilon_n$ is the nominal strain range in the member and $\Delta\epsilon_{na}$ and $\Delta\epsilon_{nb}$ are the ranges of the nominal strains due to the axial force and the bending moment in the member, respectively. The stress and strain ranges at the hot spots must follow the cyclic stress-strain relationships of the materials,

$$\Delta\epsilon = \Delta\sigma / E + C_p (\Delta\sigma / E C_e)^{K_p / K_e} \quad (4)$$

where C_e , C_p , K_e , and K_p are the material constants that were used in the Manson-Coffin's fatigue model.

The calculations of K_t 's of the fatigue specimens are shown in Table 2. The cyclic stress-strain curve used here was taken from the results of the strain-controlled cycling tests on various structural steels[2] and are those at the stage before the cyclic strain hardening took place. The K_t 's thus determined scatter widely partly because the extrapolation procedure was included in the analysis. The mean values of K_t 's were used in the fatigue analysis.

The stress measurements on the full-scale joints were carried out. The specimen is one segment of the leg where the member lengths are scaled down 1/2 from the actual structure. The three chord ends were welded to a test rig and a compressive force was applied to the one remaining end of the chord (See Fig. 2). The strain gage measurements were conducted on one of the corner joints and also on one of the tubular K-joints.

The highest stresses in the corner joints were observed in the brace walls at the points close to the weld toes. The highest stress concentration factor

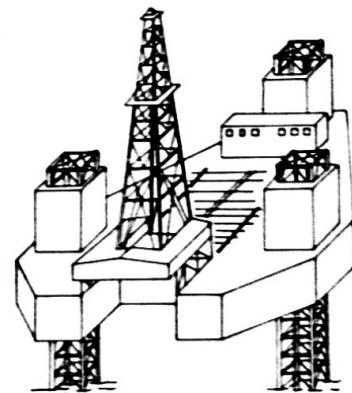


Fig. 1 Offshore Jack-Up Platform

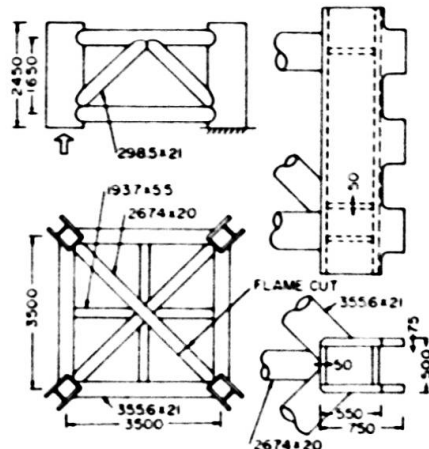


Fig. 2 Full-Scale Joint Specimen

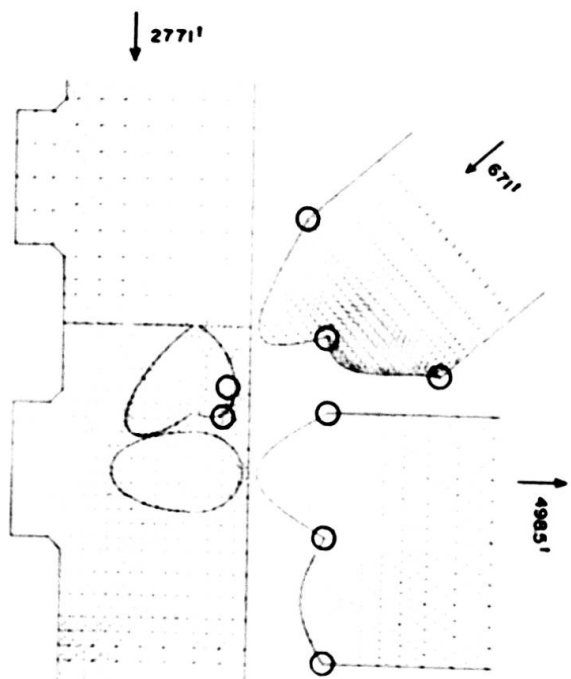


Fig. 3 FEM Analysis on Corner Joint

was 2.53. Examples of the test results are Table 1 SCF's in Corner Joint illustrated in Fig. 4.

The principal stresses in the tubular K-joints are depicted in Fig. 6. The stress concentration occurred at the points denoted by "o". The highest stress concentration factor was 2.54. It should be noted that the stress concentration factors are defined here as the "peak stress / nominal axial plus bending stresses in the brace". The stress concentration factors measured on the K-joint were found to be in reasonable agreement with the past experimental and analytical results[3], [4].

The greatest stress concentration factor of 2.8 was observed at the brace ends in the corner joint as a result of the FEM analysis (See Fig. 4). This looks to be a sufficiently conservative value and, therefore, will be used for the fatigue design being described later on.

3. Strain Range versus Life Relationships of Joints

The materials at the hot spots sustain the stress concentration due to microscopic discontinuities present at the weld toes, on top of the macroscopic stress concentration as discussed in the preceding section. The geometrical discontinuity at the weld toes has governing influences on the fatigue strength of welded joints. Even good as-welded joints are expected to have the notches with root radius of 0.02 mm, which entail the fatigue strength reduction factor of about 1.9 in mild steels[5].

It may be assumed that the fatigue strength reduction factor of the hot spot "K_f" is expressed by

$$K_f = K_t K_w \quad (5)$$

where K_w is the fatigue strength reduction factor due to the notch at the weld toe. It may be said that K_f represents the stress concentration factor of the material below the notch root at the hot spot.

The fatigue life of the material at the hot spot can be estimated from the strain histories of the material when the fatigue properties are known on the material itself. The strain in the hot spot may be calculated by K_f Δε_n in the elastic range. The strain becomes greater than this when the material yields. Such cases arise in the present joint when the structure is under storms.

One of the method to estimate the strain ranges in the hot spots is to use the Neuber's formula (3) in combination with the cyclic stress-strain relationships (4), where K_t should be replaced by K_f whenever the fatigue problem is concerned. Although the applicability of the Neuber's formula is debatable, the foregoing method was found to agree with the test results on simple notched specimens[6], [7].

Mitsui applied the above method to estimating the fatigue lives of tubular T-joints[8], [9]

| member | load case | average stress* | highest principal stress* | SCF** |
|------------------|-----------|-----------------|---------------------------|-------|
| column | 1 | -29.8 | -58.7 | 1.97 |
| | 2 | -35.7 | -65.3 | 1.83 |
| diagonal brace | 1 | -26.5 | -65.3 | 2.46 |
| | 2 | -26.5 | -61.6 | 2.33 |
| horizontal brace | 1 | 16.8 | | |
| | 2 | 19.8 | 48.2 | 2.44 |

*in kg/mm² ** SCF = highest stress / average stress

Table 2 SCF's of Fatigue Specimens

| type of specimen | Δε _n (%) | Δε (%) | Δσ (kg/mm ²) | K _t | mean of K _t 's |
|-----------------------|---------------------|--------|--------------------------|----------------|---------------------------|
| brace with heavy wall | 0.157 | 0.440 | 51.1 | 2.09 | 1.9 |
| | 0.159 | 0.480 | 52.7 | 2.18 | |
| | 0.0813 | 0.137 | 28.9 | 1.69 | |
| brace with light wall | 0.0900 | 0.128 | 26.9 | 1.42 | 0.46 |
| | 0.0920 | 0.184 | 38.8 | 2.00 | |
| | 0.0863 | 0.153 | 32.1 | 1.77 | |
| with gusset plates | 0.140 | 0.217 | 37.1 | 1.40 | 2.3 |
| | 0.156 | 0.395 | 49.1 | 1.95 | |
| | 0.0698 | 0.270 | 41.7 | 3.19 | |
| | 0.0779 | 0.219 | 37.3 | 2.54 | 0.77 |

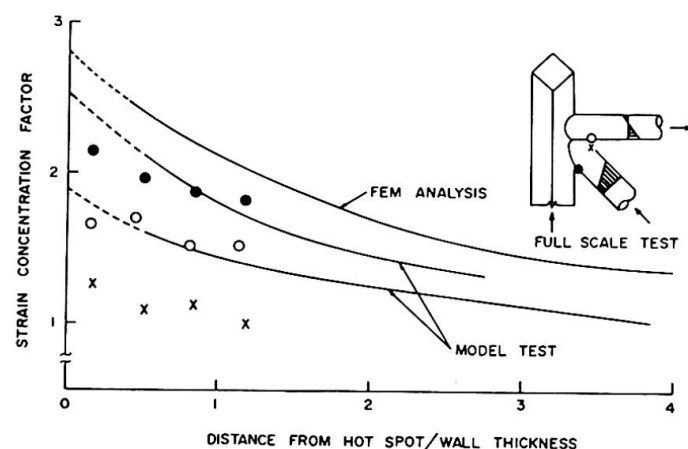


Fig. 4 Strain Distribution in Corner Joint

and found that the predicted fatigue lives fell between the cycles to crack initiation and to complete failure of the joints.

The strain ranges of the model joints were calculated by the same method. The results are shown in Fig. 7. In these tests the crack initiation was monitored by strain gages mounted on the critical points. The length of initiating cracks was less than 5 mm. K_w was assumed to be 2.0 in the calculations. The predicted fatigue curve in Fig. 7 is the S-N curve of a low carbon steel where N is the number of cycles to failure of the polished hour-glass type specimen. The fatigue constants of the material were evaluated from the static tension test results of the material and also on references to the past test results [10], [11].

Although the fatigue lives of the joints to crack initiation were less than the predicted fatigue lives, the longevities of the joints to failure were greater than the predicted lives.

The same calculations were carried out on tubular K-joints, in which K_w was assumed to be

1.9 for the specimens with the extended braces and 2.0 for the overlapping braces.

K_t were derived from the other sources [3],

[4]. The test results of these joints has already been reported elsewhere [12]. As seen in Fig. 8, the predicted fatigue lives are even less than the fatigue lives to crack initiation. It should be noted here that the first cracks were observed when they were about 20 mm long.

Zirn suggested basing on extensive tests on tubular joints that K_w was about

2 and that the S-N curves of the materials would predict the cycles to initiation of a crack of 5 mm in length [3]. The test results presented here were less consistent in this regard than the Zirn's results. This may be owing to the great diversity of weld profiles that is inherent in the as-welded joints [5]. The cycles to failure of the joints, however, were found to be apparently greater than the predicted fatigue lives.

The above method is sufficiently conservative and may be used for a design tool as far as an appropriate value of K_w is found.

4. Design of Structure against Cumulative Fatigue

The dynamic response analysis of the structure under random waves was conducted using the

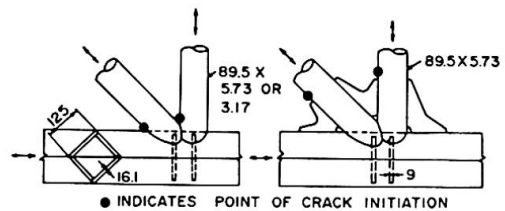


Fig. 5 Model Joints

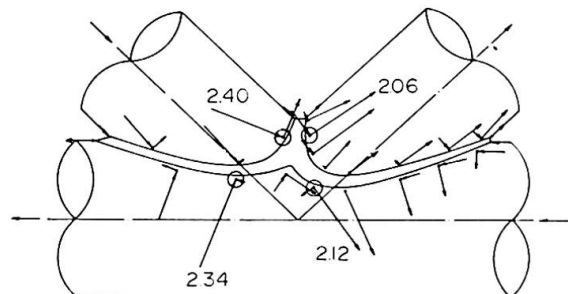


Fig. 6 Principal Stresses in Tubular K-Joint

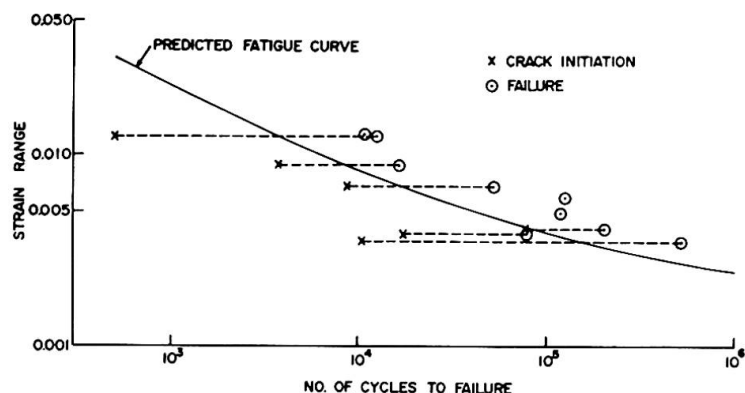


Fig. 7 Fatigue Test results on Model Joints

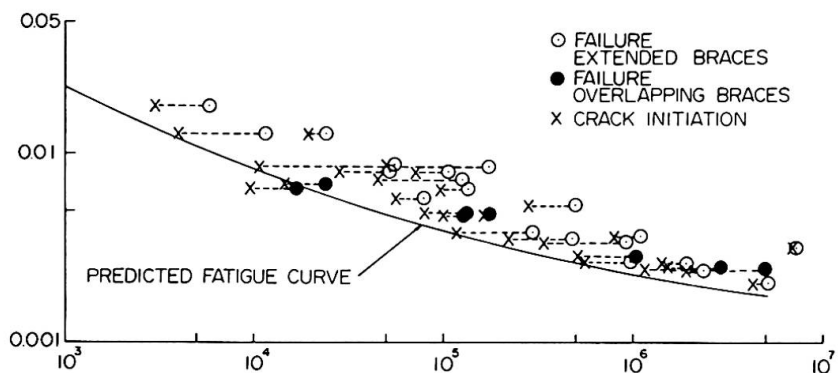


Fig. 8 Fatigue Test Results on Tubular K-Joints

probabilistic method, which would be described in detail in Reference[13]. The wind and tide forces were assumed to act statically on the structure. Table 3 shows the environmental design loads due to storms for a service period of 15 years. The storms were assumed to arise 1.5 times per year.

Fig. 9 illustrates the wave spectrum, the transfer function of the structure and the displacement response spectrum $S_{uu}(\omega)$ at the center of gravity of the deck under the wave forces. Fig. 10 depicts the frequencies of the hot spot strain ranges in 15 years, where the calculations were made with fatigue strength reduction factor of $2.8 \times 2 = 5.6$ (See Section 3).

The design fatigue curve assumed here is the S-N curve of the material in which the factor of safety of 20 is considered on the fatigue life. Such design curve is illustrated in Fig. 10. It is not advisable to use the load factor and to increase the stresses, because this tends to exaggerate the effects of low-cycle fatigue.

When the Palmgren-Meiner fatigue model is assumed, the cumulative fatigue damage ratio is calculated as follows:

$$\Sigma (n/N)_{\text{wave}} + \Sigma (n/N)_{\text{wind}} + \Sigma (n/N)_{\text{tide}} = 0.342 + 0.000 + 0.001 = 0.343$$

From the above ratio the total factor of safety assumed on the life results in 58, which suggests that the design is fairly safe against fatigue failures.

Table 3 Design Load Conditions

| | |
|----------------------------------|------|
| significant wave height (m) | 7.0 |
| significant wave period (sec) | 7.5 |
| average wind velocity (m/sec) | 25.0 |
| maximum current velocity (knots) | 4.0 |

References

1. H. Neuber, "Theory of Stress Concentration for Shear Strained Prismatic Bodies with Arbitrary Non-Linear Stress-Strain Law," Trans. ASME., J. App. Mech., Vol. 28, No. 4 (Dec. 1961)
2. Y. Kurobane, et al., "Hysteresis curves of Structural Steels-Mathematical Representations," Summary Papers, Annual Conf. of AIJ (Oct. 1975), in Japanese
3. R. Zirn, "Schwingfestigkeitsverhalten geschweißter Rohrknotenpunkte und Rohrlaschenverbindungen," Tech.-wiss. Ber. MPA Stuttgart (1975) H.75-01
4. J. G. Kuang, et al., "Stress Concentration in Tubular Joints," OTC 2205 (May 1975)
5. K. Takahashi, et al., "Effect of External Geometry of Reinforcement on the Fatigue Strength of a Welded Joint," J. JWS, Vol. 40, No. 8 (Aug. 1971), in Japanese
6. R. M. Wetzel, "Smooth Specimen Simulation of Fatigue Behavior of Notches," J. Materials, Vol. 3, No. 31 (Sept. 1968)
7. J. H. Crews, Jr., "Elasto-plastic Stress-Strain Behavior of Notch Root in Sheet Specimens under

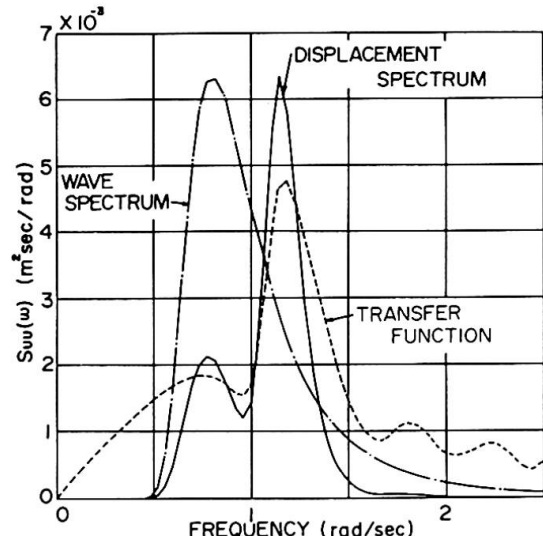


Fig. 9 Displacement Spectrum

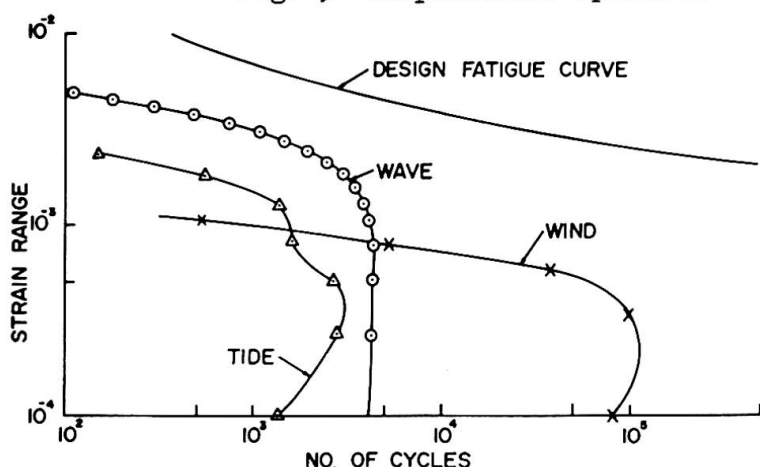


Fig. 10 Strain History Curves

- Constant-Amplitude Loading," NASA TDN 5253 (1969)
8. Y. Mitsui, Experimental Study on Local Stresses and Strength of Tubular Joints," Doctorial Dissertation, Osaka Univ. (Dec. 1973), in Japanese
 9. Y. Mitsui, "Estimation of Fatigue Life to Crack Initiation of Tubular T-Joints," Summary Papers, Annual Conf. of AIJ (Oct. 1974), in Japanese
 10. T. Hotta, et al., "Further Investigation on Estimation of Low-cycle Fatigue Strength of Steels (3rd Report)," J. SNAJ, No. 128 (Dec. 1970), in Japanese
 11. S. Klee, "Das zyklische Spannungs-Dehnungs-und Bruchverhalten Verschiedener Stähle," Veröffentlichungen des Instituts für Statik und Stahlbau der Technischen Hochschule Darmstadt, H. 22 (1973)
 12. Y. Kurobane, et al., "Some Simple S-N Relationships in Fatigue of Tubular K-Joints," Trans. AIJ, No. 212 (Oct. 1973)
 13. T. Atsuta, et al., "Fatigue Design of an Offshore Structure," OTC (1976) to be issued

SUMMARY

The fatigue life of welded joints in the offshore jack-up platform was estimated from the strain range of the material at local portions where stresses concentrated. The estimation was found to be conservative when the geometrical discontinuity at the weld toes was adequately taken into account. The fatigue design was carried out considering the cumulative damage of the joints under the influences of random wave and wind forces.

RESUME

La fatigue des joints soudés dans les plates-formes auto-élévatrices est estimée à partir des déformations du matériau aux points de concentration de contraintes. Les résultats sont du côté de la sécurité, si la forme géométrique de discontinuité à l'angle de soudure a été correctement pris en considération. Le calcul à la fatigue a tenu compte du dommage cumulatif des joints sous l'influence aléatoire des forces des vagues et du vent.

ZUSAMMENFASSUNG

Die Lebensdauer ermüdungsbeanspruchter geschweißter Stöße in selbst-hebenden Bohr-Plattformen wurde abgeschätzt in Funktion der Dehnungsschwingweite an Punkten mit Spannungskonzentrationen. Die Abschätzung liegt auf der sicheren Seite, wenn die geometrischen Diskontinuitäten im Bereich der Schweißnähte berücksichtigt werden. Der Nachweis der Ermüdungsfestigkeit wurde erbracht unter der Annahme stochastischer Wellen- und Windkräfte und fortschreitender Zerstörung.